Variability of dimethyl sulphide (DMS), methanethiol and other trace gases in context of microbial communities from the temperate Atlantic to the Arctic Ocean

Valérie Gros[1], Bernard Bonsang[1], Roland Sarda-Estève[1], Anna Nikolopoulos[2], Katja Metfies[3], Matthias Wietz[3,4] and Ilka Peeken[3]

[1] Laboratoire des Sciences du Climat et de l'Environnement, CNRS-CEA-UVSQ, IPSL, Gif sur Yvette, 91 191, France
[2] Norwegian Polar Institute, Fram Centre, 9296 Tromsø, Norway
[3] Alfred Wegener Institute Helmholtz Centre for Polar and Marine Research, 27570 Bremerhaven, Germany
[4] Max Planck Institute for Marine Microbiology, 28359 Bremen, Germany

Correspondence to: Valérie Gros (valerie.gros@lsce.ipsl.fr)

Abstract.

Dimethyl sulphide (DMS) plays an important role in the atmosphere by influencing the formation of aerosols and cloud condensation nuclei. In contrast, the role of methanethiol (MeSH) for the budget and flux of reduced sulphur remains poorly understood. In the present study, we quantified DMS and MeSH together with the trace gases carbon monoxide (CO), isoprene, acetone, acetaldehyde and acetonitrile in North Atlantic and Arctic Ocean surface waters, covering a transect from 57.2°N to 80.9°N in high spatial resolution. Whereas isoprene, acetone, acetaldehyde and acetonitrile concentrations decreased northwards, CO, DMS and MeSH retained significant levels at high latitudes, indicating specific sources in polar waters. DMS was the only compound with higher average in polar (31.2 ± 9.3 nM) than in Atlantic waters (13.5 ± 2 nM), presumably due to DMS originating from sea ice. At eight sea-ice stations north of 80°N, in the diatom-dominated marginal ice zone, vertical profiles showed a marked correlation ($R^2 = 0.93$) between DMS and chlorophyll a. Contrary to previous measurements, MeSH and DMS did not co-vary, indicating decoupled processes of production and conversion. The contribution of MeSH to the sulphur budget (represented by DMS+MeSH) was on average 20% (and up to 50%) higher than previously observed in the Atlantic and Pacific Oceans, suggesting MeSH as a significant source of sulphur possibly emitted to the atmosphere. The potential importance of MeSH was underlined by several correlations with bacterial taxa, including typical phytoplankton associates from the *Rhodobacteraceae* and *Flavobacteriaceae* families. Furthermore, the correlation of isoprene and chlorophyll a with *Alcanivorax* indicated a specific relationship with isoprene-producing phytoplankton. Overall, the demonstrated latitudinal and vertical patterns contribute to the understanding of central marine trace gases from chemical, atmospheric and biological perspectives.

1 Introduction

Volatile Organic Compounds (VOCs) and carbon monoxide (CO) are important in atmospheric chemistry as precursors of ozone and secondary organic aerosols, which affect air quality and climate. The oceans become increasingly considered as

35   source and sink of CO and VOCs with potential influence on atmospheric chemistry, despite globally remaining a small source compared to anthropogenic emissions (Duncan et al., 2007; Kansal, 2009) and terrestrial vegetation (Guenther et al., 1995). Biological activities substantially contribute to the dynamics of short-lived VOCs like dimethyl sulphide (DMS) and isoprene. For instance, dimethylsulfoniopropionate (DMSP) produced by phytoplankton can be metabolized by bacteria into DMS (Stefels et al., 2007). DMS is rapidly oxidized once emitted to the atmosphere, then representing a major precursor of sulphate

40   aerosols with radiative impacts by scattering sunlight and constituting condensation nuclei (Galí et al., 2021 and references therein). Alternatively, DMSP can be microbially demethylated into methanethiol (CH_3SH, herein referred to as MeSH), whose role in the atmosphere and oceans is poorly characterized to date (Lawson et al., 2020). The oxidation of MeSH by hydroxyl radicals OH effectively produces SO_2, with up to 48% based on model calculations (Novak et al., 2021). Thus, MeSH is probably an underestimated factor in the marine gaseous sulphur cycle.

45   Isoprene, another important trace gas, can be produced by photosynthesizing organisms over short timescales (a few hours), with potential influence on regional atmospheric chemistry and aerosol formation above biologically active pelagic waters (Bikkina et al., 2014). Photosynthetic cyanobacteria are stronger emitters of isoprene than diatoms, with taxon-specific variability in production (Bonsang et al., 2010; Shaw et al., 2010). Besides direct emission by primary producers, oceanic trace gases can originate from photochemical processes. For instance, photodegradation of dissolved organic matter is the main

50   source of CO (Wilson et al., 1970), although laboratory experiments showed a minor contribution of biological activities (Gros et al., 2009).

The way oceanic areas contribute to the budget of oxygenated VOCs (OVOC) is also important to consider, since these compounds may affect the oxidative capacity of the remote atmosphere through the budget of tropospheric radicals. A recent study has confirmed the importance of air-sea exchange for acetaldehyde, pointing out the lack of oceanic measurements

55   (Wang et al., 2019). In the budget of these organic species, marine waters can be either local source or sink depending on the region. Acetone is considered to originate from photodegradation of dissolved organic carbon (Zhou and Mopper, 1997). A positive net flux of acetone is generally observed in biologically productive areas such as tropical upwelling zones, whereas a sink occurs at high latitudes or in oligotrophic waters (Lawson et al., 2020). Furthermore, the OVOCs acetone, methanol, acetonitrile and acetaldehyde can show seasonal variation (Davie-Martin et al., 2020).

60   Linking the dynamics of VOCs and trace gases to primary production and microbial distribution helps understanding fundamental couplings between biological, oceanic and atmospheric processes. This is particularly important in the Arctic Ocean, which warms two to three times faster than the global average (Schmale et al., 2021 and references therein). These

processes concur with changing physical, biological and photochemical parameters, subsequently affecting the coupling between ocean and atmosphere. Importantly, sea ice melt influences the production of VOCs, e.g. through increased primary

65   production in ice-free waters (Arrigo and van Dijken, 2015), release of ice algae and their substrates (Fernández-Méndez et al., 2014), as well as higher gas exchange at the ocean-atmosphere interface when ice-free areas expand (Lannuzel et al., 2020). Concurrent changes in phytoplankton distribution can amplify these dynamics, for instance linked to the northward expansion of the coccolithophorid *Emiliania huxleyi* by Atlantic currents (Hegseth and Sundfjord, 2008) and changing bloom phenologies (Nöthig et al., 2015; von Appen et al., 2021). As phytoplankton and bacterial distribution are often linked, these dynamics

70   subsequently affect the heterotrophic food web. The bacterial families *Rhodobacteraceae* and *Flavobacteriaceae* are frequently abundant during phytoplankton blooms, contributing to the degradation of algal organic matter and the conversion of DMSP into DMS and MeSH (Moran et al., 2012; Moran and Durham, 2019). Campen et al., (2022) have recently emphasized the need to better link bacterial distribution with DMS and CO metabolism. In addition, the bacterial degradation of e.g. isoprene might be an important, yet understudied contribution to biogeochemical cycles (Carrión et al., 2020).

75   Contextualizing marine VOCs, trace gases and microbes in Arctic vs temperate Atlantic waters is important, as Atlantic characteristics expand northward with climate change (Polyakov et al., 2020). Here, we report concentrations of DMS, MeSH, isoprene, CO, acetone, acetaldehyde and acetonitrile in context of microbial distribution across the North Atlantic and Arctic Oceans. During the TRANSSIZ campaign on-board RV Polarstern from early spring to summer 2015, we continuously measured these compounds in surface waters between 57° to 80°N, and additionally over vertical profiles from the surface to

80   50 m depth in the ice-covered region north of Svalbard (Fig. 1). The main objective was to document the levels and spatial variability of trace gases, specifically the ratio between MeSH and DMS, in context of phytoplankton numbers, bacterial diversity, water masses and sea ice cover. To our knowledge, this is the first survey of MeSH in the Arctic Ocean, shedding light on its biogeochemical role in an area of rapid climate change.

2 Material and methods

85   ### 2.1 Campaign description and oceanographic parameters

Water samples were collected during the TRANSSIZ ("Transitions in the Arctic Seasonal Sea Ice Zone"; PS 92 - ARK XXIX/1) cruise on-board RV Polarstern between May 19th and June 28th, 2015. The cruise started in Bremerhaven, Germany, and ended in Longyearbyen, Svalbard (Fig. 1), as described in detail by Peeken (2016).

Along the ship track between May 19th and 27th, trace gases were continuously measured in the surface water layer. Salinity,

90   temperature and chlorophyll a (Chl a) fluorescence were continuously measured with the FerryBox System of the Helmholtz-Zentrum Geesthacht (HZG) in surface water (6 m depth). The instrument performs a self-cleaning routine every day with acid washing and freshwater rinsing. Usually no drift of the sensors is observed (for details see Petersen (2014)). Temperature,

salinity and Chl a were extracted from the database every 2 minutes. The sensor for Chl a was a submersible fluorometer (Turner Designs, Sunnyvale, CA, USA) with excitation/emission wavelengths of 325 nm and 425 nm respectively.

95 After May 27th, eight ice stations (number 19, 27, 31, 32, 39, 43, 46, and 47, Table S1) were carried out over the continental shelf north of Svalbard and over the Yermak Plateau (Fig. 1; Table S1). At each ice station, the ship was anchored to an ice floe at drift for approximately 36 h. While carrying out ice work on the port side, winch-operated instruments were deployed in the open water on the starboard side to record biological and biogeochemical variables including trace gases and phytoplankton pigments. Except for the first ice station (in 70% ice cover and still some leads present), the stations were
100 conducted in almost 100% ice cover (Massicotte et al., 2019) with the sampling taking place in small leads. All ice stations were 50 to 250 km away from the ice edge and open water (Dybwad et al., 2021). A detailed study of nutrients, marker pigments and protist microscopy classified the Yermak Plateau stations (39, 43, 46) to be in a pre-bloom phase, while all other stations were in a bloom phase (Dybwad et al., 2021). During the ice stations, discrete seawater samples for trace gas and phytoplankton composition analysis were collected at six different depths of the water column using the CTD (conductivity,
105 temperature, depth) water-sampling carousel. These samples were collected in 1 L light-proof flasks for direct analysis on board. Values for temperature and salinity were provided by the CTD bottle data file for each station (Nikolopoulos et al., 2016).

Temperature and salinity from both types of sampling were used to classify the sampled water masses based on the criteria applied in Tran et al., 2013 (Table1).
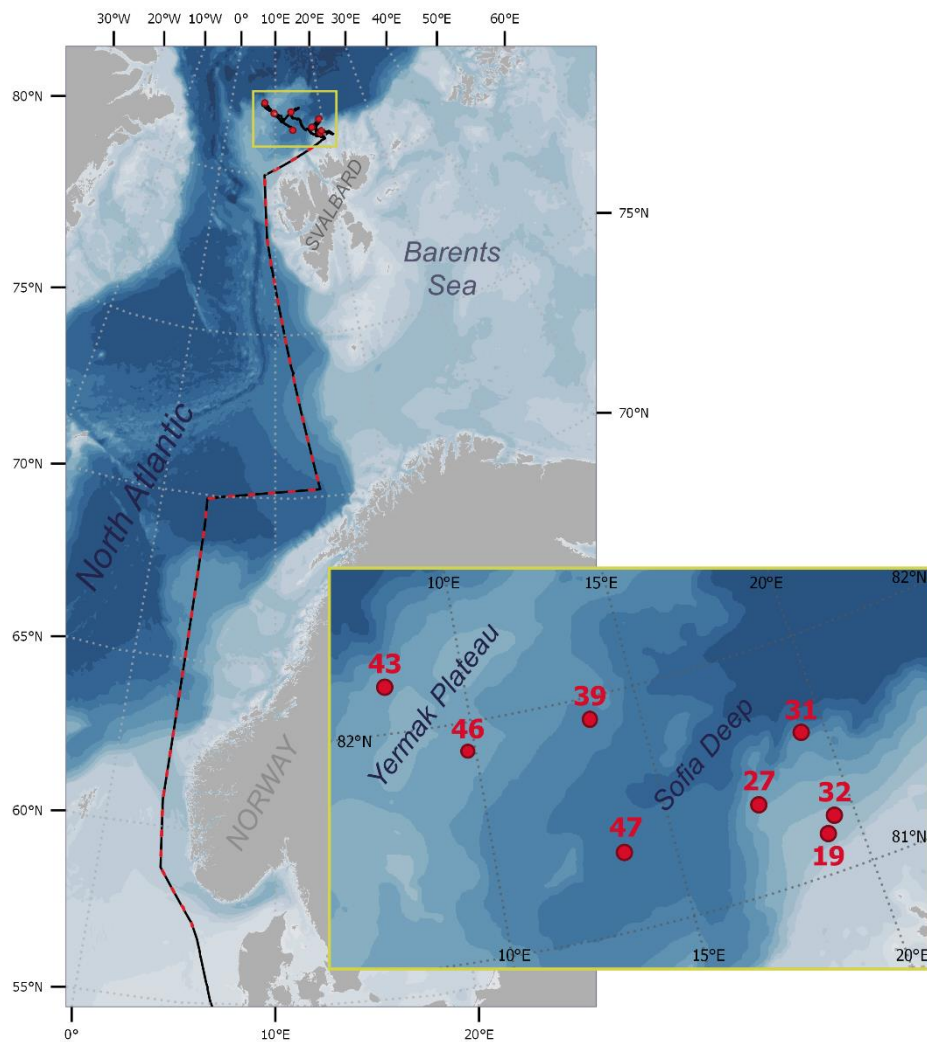
110

Fig. 1. Overview of the campaign ship track (black solid line). Surface measurements were sampled by the FerryBox system between 57ºN and 81ºN (dashed red line). Vertical profiles were sampled at eight sea ice stations (yellow insert; Table S1).

115

2.2 Biological measurements.

2.2.1 Pigment analysis

For pigment analysis with high pressure liquid chromatography (HPLC), seawater samples (1–2 L) were taken from Niskin
120 bottles mounted on a CTD rosette from six depths in the upper 50 m (Table S1). All samples were analysed within few hours after collection.

5

Sample handling and pigment measurements were carried out as described in Tran et al. (2013). The FerryBox/surface Chl a data were calibrated against surface Chl a l concentrations derived from Niskin bottles ($R^2 = 0.84$, see Fig. S1). The taxonomic composition of phytoplankton was calculated from marker pigments using the CHEMTAX approach (for details see
125 Wollenburg et al., (2018)), distinguishing diatoms, *Phaeocystis*-type haptophytes, prasinophytes, chlorophytes, dinoflagellates, cryptophytes, chrysophytes and coccolithophorid-type haptophytes. The contribution of each group was expressed as Chl a concentrations.

2.2.2 Bacterial community analysis

In total 34 seawater samples for bacterial community analysis were collected along the transect (Table S2) at a depth of ~10
130 m using the AUTOFIM system (Metfies et al., 2016, 2020), which is installed at the bow of RV Polarstern next to the ship's pump system intake. Per sampling event, two liters of seawater were filtered onto polycarbonate filters with 45 mm diameter and 0.4 µm pore size (Millipore; USA) at 200 mbar. Filters were stored at -80°C until DNA extraction in the home laboratory using the NucleoSpin Plant II kit (Macherey-Nagel, Germany) according to the manufacturer's instructions. Bacterial 16S rRNA gene fragments were amplified using primers 515F–926R (Parada et al., 2016) according to the 16S Metagenomic
135 Sequencing Library Preparation protocol (Illumina, San Diego, CA). Amplicon gene libraries were sequenced using Illumina MiSeq technology in 2x300 bp paired-end runs at CeBiTec (Bielefeld, Germany). Raw sequence files have been deposited in the European Nucleotide Archive under accession number PRJEB50492, using the data brokerage service of the German Federation for Biological Data (GFBio) in compliance with MIxS standards. The complete amplicon analysis workflow is described in Supplement S2, with Rscripts documented under https://github.com/matthiasswietz/transsiz. Briefly, after primer
140 removal using cutadapt (Martin, 2011), reads were classified into amplicon sequence variants (ASVs) using DADA2 (Callahan et al., 2016) and taxonomically classified using the Silva v138 database (Quast et al., 2012). We obtained on average 85,000 quality-controlled, chimera-filtered reads per sample (Table S2) sufficiently covering community composition (Fig. S2).

2.3 Trace gas measurements

Carbon monoxide and VOCs dissolved in seawater were measured in real-time along the transect using samples from the
145 Ferrybox water intake (6 m depth). Seawater was delivered by the ship membrane pump to the laboratory for continuous injection into an online water extraction device (OLWED; Supplement S3, Fig. S3). Furthermore, we measured trace gas concentrations from the surface (0.5 m) to 50 m depth at the eight ice stations, analysing all samples within few hours after collection. Possible causes of artefacts during this storage period have been investigated in a previous experiment in the same area (Tran et al., 2013), showing no significant losses of low molecular weight VOCs and a slow decrease for CO during the
150 first 4 hours (Xie and Zafiriou, 2009 and Tolli and Taylor, 2005).

2.3.1 PTRMS measurements

VOC were quantified using a high sensitivity Proton-Transfer Mass Spectrometer (PTRMS, Ionicon Analytik) developed by (Lindinger and Jordan, 1998) and since then widely used (see for example review by Blake et al., (2009)). This instrument principle is based on the soft chemical ionization of VOCs by proton-transfer. This proton-transfer reaction is possible for all

155 compounds having a proton affinity higher than the one from water, giving access to a large variety of VOCs. The soft ionization allowing only small fragmentation, the compounds are directly measured at their at their corresponding m/z+1. During the campaign, air from the headspace was continuously sampled by the PTRMS through a ⅛ inch PFA line at a flowrate of about 60 ml/min using usual parameters, i.e. 60°C (inlet and drift tube temperature), 600V drift tube and 2.2 mbar drift tube pressure (with a corresponding E/N of 132 Td, towsend). Measurements were usually performed every 2.5 minutes, except for

160 a short period (from 61.1 °N to 65.3°N, representing about 24 h), when they were only performed every 10 min in order to scan a wider range of masses (m/z) on the PTRMS and to select the compounds of interest, i.e. showing a signal above the detection limit. After this, about 25 masses (m/z) were selected to be further monitored (with dwell times from 1 to 20 s) and this paper presents the results for the compounds showing the most significant variability, i.e. isoprene, dimethyl sulphide, methanethiol, acetone, acetaldehyde, and acetonitrile. The calibration procedures (in the gas and water phases) are given in

165 Supplement S4, Figures S4 and S5.

2.3.2 CO measurements

CO was measured using a custom-made gas chromatograph directly coupled to the extraction cell and equipped with a hot mercuric-oxide detector operating at 265°C (RGA3, Trace Analytical, Menlo Park, CA, USA). The system comprised two 1-mL nominal volume stainless-steel injection loops (for samples and calibration, respectively), previously calibrated in the

170 laboratory. The chromatographic procedure used a pre-column (0.77m length, 0.32 cm outer diameter, containing Unibeads 1S 60/80 mesh) and an analytical column (0.77m length, 0.32 cm outer diameter, containing molecular Sieve 13X 60/80 mesh) both heated to 95°C. Air sample (from the headspace of the extraction cell) and standard gas were alternately injected into the chromatograph, each sample being directly calibrated with the previous injection of the standard gas. The standard gas consisted of CO diluted in synthetic air at a nominal concentration of 200 ppbv. The CO retention time was 1.5 min, and a

175 complete chromatogram ran for 2.5 min. The overall accuracy of the measurement was about 5%. More details about CO measurements can be found in Gros et al. (1999) and Tran et al. (2013).

3 Results

3.1 Latitudinal variability in surface waters from 57°N to 80°N

180 Along the latitudinal transect, we performed online measurements of Chl a and hydrographic parameters, covering five different water masses: warm Atlantic Water with low salinity (AWs), 'regular' warm Atlantic Water (wAW), freshened and cooled Atlantic Water (fAW), cold Polar Water (cPW) and warm Polar Water (wPW) as defined in Table 1 following Tran et al. (2013). The major part of the transect, from 63 to 80°N, occurred in wAW (see Fig. S6). Fresher (low-saline) Atlantic Water (AWs and fAW) were mainly encountered where the Norwegian Atlantic Slope Current waters meet the coastal-influenced,

185 fresher water masses of the Norwegian Coastal Current (cf. Fig.1 of Skagseth et al., (2022)): AWs at 60.6-62.3 °N (with fAW in the mixing zones) , and fAW around 70-72°N. Polar Water only occurred north of 80°N.

Surface temperature steadily decreased northwards, from 8°C to below 0°C in the ice-covered region >80°N (Fig. 2). The slight deviation around 70°N corresponds to the shifting cruise track towards Tromsø due to a medical evacuation event (cf. Fig. 1). Chl a concentrations peaked at the beginning of the transect, with overall five areas where concentrations exceeded

190 1 µg L^{-1} indicating increased phytoplankton abundances: ~ 60°N to 61°N (up to 2 µg L^{-1}), several locations >66°N (>6-8 µg L^{-1}), and three additional peaks (>5 µg L^{-1}) at 76°, 78°, and 79.5°N, respectively. Within the marginal ice zone (>80°N) Chl a concentrations reached up to 3 µg L^{-1}.

3.1.1 Trace gas distribution

The oxygenated gases acetone and acetaldehyde strongly decreased with higher latitudes and lower water temperatures, being

195 below or close to the detection limit >70°N. Nevertheless, we observed a 2- to 3-fold increase between 61°N and 65°N. Acetone varied from 20 to 25 nM between 57 to 65°N, decreasing to 0.1 nM near 80°N. A maximum of 40 nM between 60°N and 65°N covaried with higher Chl a concentrations, plus a second minor peak between 77°N and 79°N. Similar latitudinal trends occurred for acetaldehyde and acetonitrile. Acetaldehyde decreased from 15 nM in the temperate Atlantic to 0.5-3 nM in the Arctic Ocean, with a peak of approx. 40 nM between 60°-65°N. Acetonitrile decreased from 1.5 nM to 0.1-0.5 nM, with a

200 second maximum of approx. 2 nM between 60° and 65°N. Isoprene decreased from 4-5 pM at 57°N to 0.3-1.5 pM at 80°N, with three additional maxima along the transect. Opposed to the other trace gases, isoprene slightly increased again north of 80°N, albeit at a much lower concentration compared to lower latitudes.

CO, DMS and MeSH displayed different patterns, retaining high but variable concentrations at high latitudes. CO concentrations varied between 2 and 30 nM, with several peaks covarying with Chl a at 62.5, 67 and 77.6°N. DMS ranged

205 from ~2 nM to 50 nM, with peaks occurring at 61-63°N, 66-70.5°N and a maximum of 60 nM at 80°N. MeSH varied from 0.1 to 7 nM, with concentration peaks near 70°N and between 73-75°N.
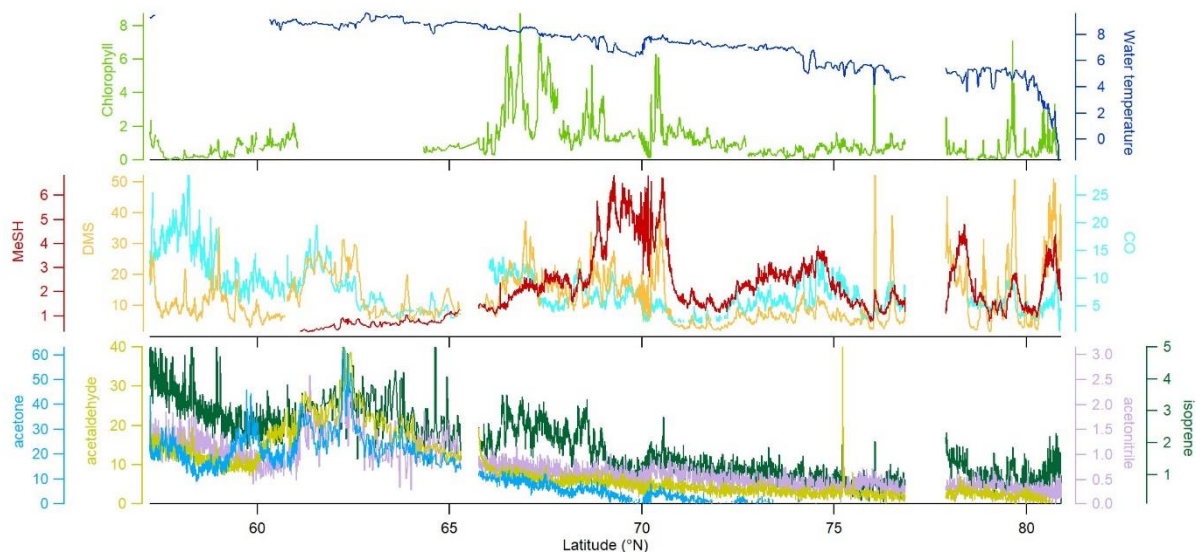
Figure 2: Latitudinal variability of acetone (nM), acetaldehyde (nM), acetonitrile (nM), isoprene (pM), DMS (nM), MeSH (nM), and CO
(nM) between 57.2°N to 80.9°N in relation to Chl a (µg L^{-1}) and water temperature (°C). Due to sensor failure temperature values are missing
until ~61°N.

3.1.2 Bacterial communities in the environmental context

We performed 16S rRNA amplicon sequencing to characterize bacterial community structure in context of latitude, water
temperature and trace gas concentrations. Correspondent to the known microbial differences between temperate and polar
oceans (Sunagawa et al., 2015), communities substantially varied by latitude and temperature (Fig. 3). These factors explained
43% of bacterial variability (PERMANOVA; $p < 0.001$). Several correlations between trace gases, Chl a and the abundance
of specific ASVs (Fig. 3) suggests bacterial linkages with phytoplankton blooms and VOC conversion. Correlations were both
positive and negative, sometimes differing within single genera. For instance, one SAR92-ASV positively correlated with
MeSH, whereas another SAR92-ASV negatively correlated with DMS. For MeSH and its ratio to DMS, correlations differed
between *Pseudofulvibacter*, NS10, OM75, *Yoonia-Loktanella* and *Ascidiaceihabitans* ASVs (negative) versus SUP05
(positive). Interestingly, we detected negative correlations of *Synechococcus* and another cyanobacterial ASV with MeSH.
DMS positively correlated with ASVs from *Aurantivirga* and SAR11 clade Ia. Two ASVs from the NS9 clade were unique in
their correlations with acetone and acetonitrile. Furthermore, several ASVs from *Thalassolituus* and *Alcanivorax* (negative),
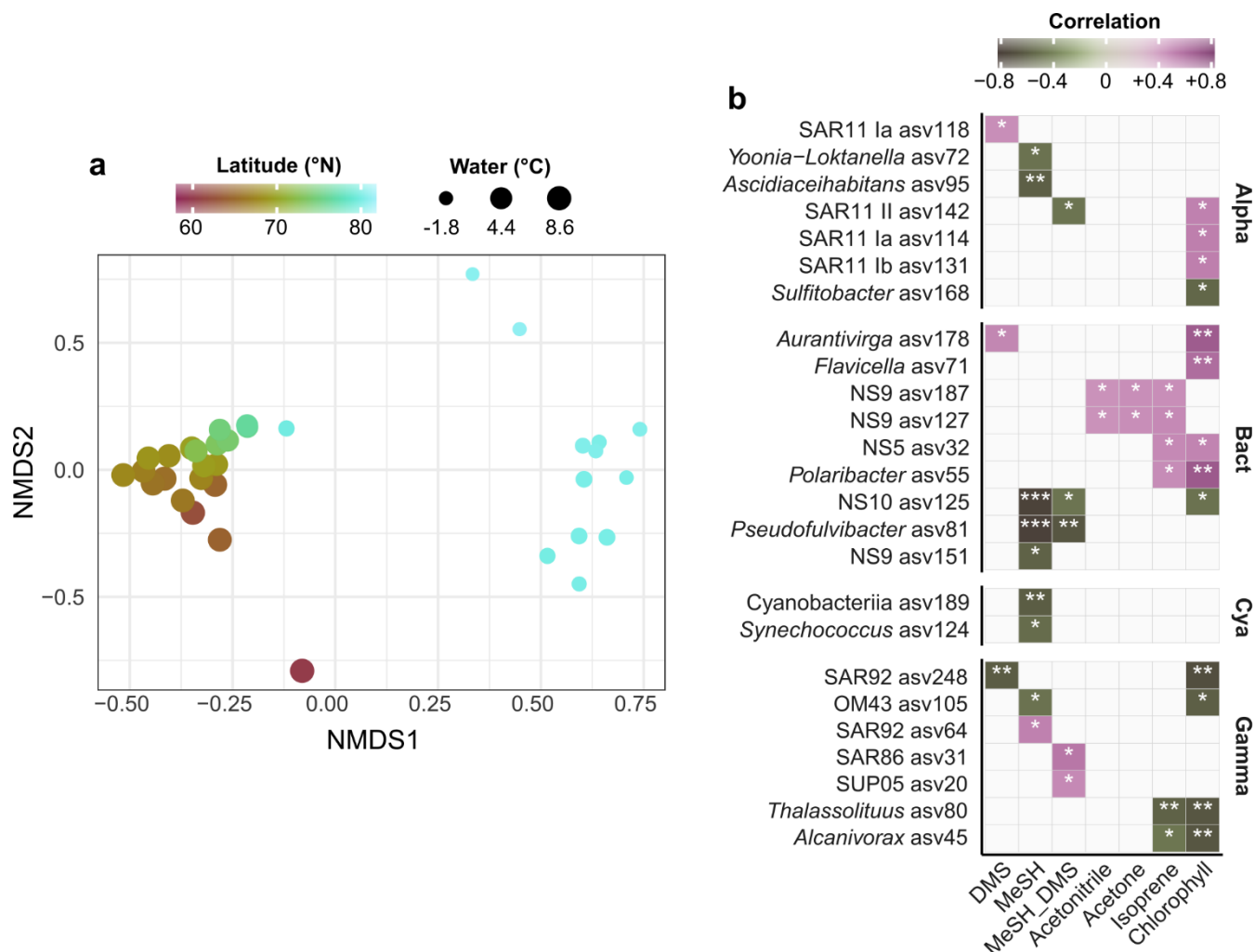NS5 and *Polaribacter* (positive) correlated with Chl a and isoprene.

Fig. 3. a) Nonmetric multidimensional scaling of bacterial community composition (Bray-Curtis dissimilarities of Hellinger-transformed relative abundances). The colour gradient and dot size illustrate latitude and water temperature respectively. b) Spearman correlations between environmental parameters and the abundance of bacterial ASVs. Only correlations >|0.4| are shown, and only if stronger than with latitude. No correlations occurred with acetaldehyde and CO. Alpha: Alphaproteobacteria; Gamma: Gammaproteobacteria; Bact: Bacteroidetes; Cya: Cyanobacteria. Asterisks indicate Holm-corrected p-values (* < 0.05; ** < 0.01; *** < 0.001).

3.2 Vertical under-ice profiles north of 80°N

In the ice-covered region north of Svalbard, the continuous surface seawater measurements were changed to vertical under-ice profiles at eight stations (Fig. 1, 4, Fig. S7). To connect latitudinal with vertical data, we compared the cPW values measured along the transect with the surface values from the vertical profiles (Tab. 2, Fig. 4). This revealed marked differences in trace gas concentrations compared to the polar water masses along the transect, except for acetonitrile. Acetaldehyde concentrations

(0.3 to 14.2 nM with an average of 7.2 ± 4.4 nM for surface values, i.e. 0.5 m under water) were much higher than in polar waters in the northern part of the transect (0.8 ± 2.0 nM) and more in the range of the previously described wAW (4.8 ± 4.0

240　nM) and fAW (9.8 ±5.6 nM). A similar increase was apparent for acetone, with values closer to wAW than to polar waters. DMS varied substantially (from 1.6 to 31.9 nM for the surface values) at the sea-ice stations. For DMS the bloom stations 19 and 32 (see section 2.1 and Dybwad et al., 2021) were in the range of the previously described polar waters, but particularly the pre-bloom stations (39, 43, 46) only showed >2 nM DMS for surface values. MeSH and CO both exhibited lower concentrations (0.13 ± 0.17 nM and 1.45 ± 1.67 nM respectively) at the sea-ice stations. In contrast, isoprene concentrations

245　were higher (3.2 ±2.1 pM) at the sea-ice stations compared to all other water masses along the transect. The marked difference between polar waters observed in the northern part of the transect and surface values from sea-ice stations was also evident in Chl a, marker pigments of relevant phytoplankton groups (diatoms and *Phaeocystis*), and some trace gases (DMS, MeSH, CO, isoprene) over the entire depth profile. The shallow shelf stations 19 and 32 were characterized by a marked phytoplankton bloom with up to 10 µg L^{-1} of Chl a, dominated by up to 90% by diatoms, indicating a typical spring bloom scenario (Degerlund

250　and Eilertsen, 2010). At the pre-bloom stations 39, 43 and 46, low biomass (Chl a < 0.5 µg L^{-1}) coincided with a mixed pico- and nanophytoplankton community including prasinophytes, chlorophytes, dinoflagellates, cryptophytes, chrysophytes and coccolithophorid-type haptophytes (Fig. S7). Diatoms accounted for approximately half of the biomass at most stations. *Phaeocystis*, a typical bloom-forming organism in the high Arctic (Degerlund and Eilertsen, 2010) dominated at station 47 with up to 80% of phytoplankton biomass, but the here found concentrations were much lower compared to the under ice

255　bloom of this species found in the same region and year by (Assmy et al., 2017). This indicates already a declining bloom during our sampling period towards the end of June. Except for the Yermak plateau stations (39, 43, 46), *Phaeocystis* contributed between 10-40% of the phytoplankton biomass.

We observed a strong correlation between DMS and Chl a (R-squared Pearson's correlation coefficient = 0.93; Fig. S8), suggesting diatoms as the most prominent photosynthetic group. Isoprene and CO also markedly correlated with Chl a (R^2 =

260　0.6, Fig. S8), but only when excluding station 19. Both compounds show constant, low concentrations from the surface down to 50 m depth. Exceptions are station 32 (both compounds) and 43 (only CO), where the constant decrease with depth probably represents decreasing photochemical production following lower light penetration with depth, without additional biological production. In addition, at station 31, CO (and isoprene, although less pronounced) peaked at 30 m depth, but without prominent links to Chl a. In contrast to the values along the latitudinal transect, MeSH showed low concentrations at most ice

265　stations, except for station 19 (with higher concentrations and a clear decrease with depth) as well as at station 31 (with a small depth-maximum observed at 30 m depth comparable to CO and isoprene).

270
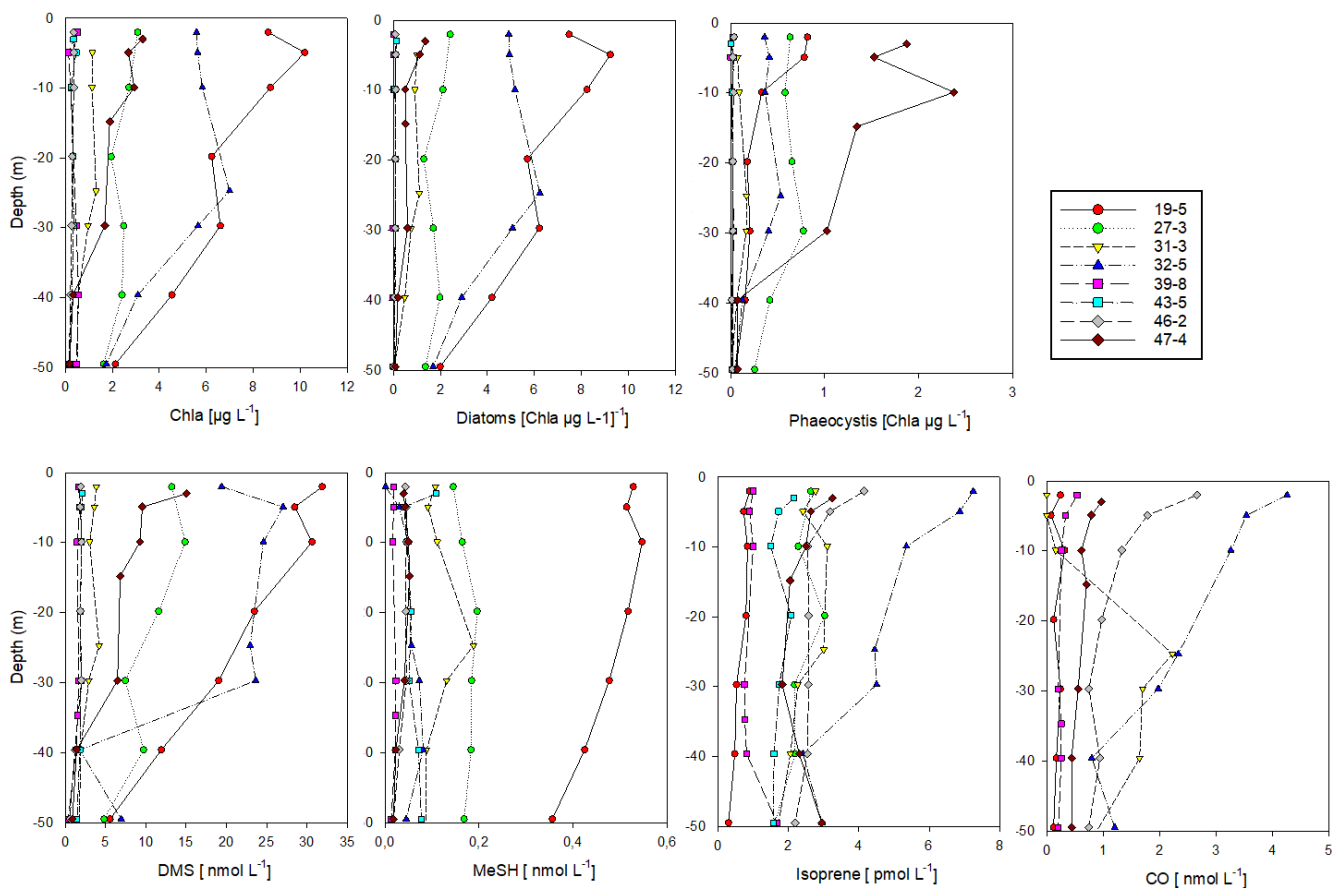
Fig. 4. Biological parameters and trace gas vertical distribution (0-50 m depth) measured at sea-ice covered stations north of 80°

4 Discussion

4.1 Isoprene, CO, acetone, acetaldehyde and acetonitrile

Our study provides a comprehensive overview of biologically and climatically relevant trace gases in the microbiological context; covering ~1400 nautical miles from 57°N to 81°N (May-June 2015) as well as under-ice vertical profiles north of Svalbard. Isoprene and CO can be compared with a previous study (Tran et al., 2013), which was carried out in June-July

2010, i.e. one month later in the summer season and in different water masses (Table 1), but where hardly any phytoplankton

blooms were encountered. Concentrations of isoprene, usually associated with phytoplankton (Bonsang et al., 1992; Shaw et

285   al., 2010), were about one order of magnitude lower than described by Tran et al. (2013), even though the biomass indicator

Chl a was overall lower (2 µg L^{-1} compared to up to 8 µg L^{-1} reported here). This may relate to seasonal differences in

phytoplankton composition, as phytoplankton taxa are known to vary their isoprene emissions (Bonsang et al., 2010; Shaw et

al., 2010). Similar seasonal differences in isoprene concentrations were observed by Hackenberg et al., (2017), reporting on

average 4.3 pM for March compared to 19.9 pM in July/August in the Arctic sector of the Pacific Ocean. Lower isoprene

290   concentrations in polar waters correspond to values from Ooki et al. (2015), who showed 27 – 33 pM in subpolar and transition

waters, and 4 pM in polar waters, respectively. With regard to the vertical profiles, the slight secondary maximum at 20-40 m

depth may correspond to the Chl a maximum, as already been found by Tran et al. (2013). Nevertheless, the concentrations

are overall much lower (about one order of magnitude) than reported by Tran et al., (2013), indicating a high spatial variability

of isoprene potentially related to seasonally varying phytoplankton abundances. Simó et al., (2022) recently highlighted the

295   importance of biological consumption of isoprene in water, possibly matching the magnitude of isoprene ventilated to the

atmosphere), advising to consider both the sources and sinks when discussing isoprene concentrations and variability. The

correlations of *Alcanivorax* and *Thalassolituus* ASVs with both isoprene and Chl a support phytoplankton as source of this

trace gas, and subsequent bacterial utilization (Alvarez et al., 2009). In this context, *Alcanivorax* has been reported during

phytoplankton blooms in the subarctic Atlantic (Thompson et al., 2020) and can degrade isoprene (Alvarez et al., 2009).

300   *Alcanivorax* and *Thalassolituus* can be associated with microalgal surfaces and also perform hydrocarbon degradation (Love

et al., 2021), indicating additional phytoplankton-linked factors that influence their distribution.

To date, CO in Arctic seawater has only been measured by Tran et al. (2013) in the same Arctic region as well as by Xie and

Zafiriou (2009) in the Beaufort Sea. For polar waters, our mean value of 5.9 ± 2.9 nM matches previously reported averages

(6.5 ± 3.2 nM for Tran et al. (2013) and 4.7 ± 2.4 nM for Xie and Zafiriou, (2009)). These concentrations are relatively high

305   compared to the global oceanic mean of 2 nM CO (Conte et al., 2019). Elevated values in the Arctic are not reproduced by the

NEMO-PISCES model, possibly attributed to the release of CO and/or coloured dissolved organic matter from sea-ice melt or

to lower bacterial consumption in cold waters (Conte et al., 2019). The first hypothesis is supported by up to 100 nM CO

measured in sea ice (Xie and Gosselin, 2005; Song et al., 2011; Boissard et al., pers. comm.). Concerning CO in Atlantic

waters, the demonstrated concentrations of up to 10.7 ± 3.1 nM are higher than in polar waters, and exceed data from the same

310   region, 5 years before (Tran et al., 2013) by up to fourfold. Highest CO values in temperate waters with low Chl a suggest that

CO could have originated from an abiotic source, e.g. the photodegradation of coloured dissolved organic matter. Only in

vertical under-ice profiles, similar trajectories of Chl a and CO suggest an additional biological source in the euphotic zone,

as already been shown by Tran et al. (2013). Biological sources of CO have extensively been studied by Gros et al., (2009),

and the missing congruency at station 19 might be explained by the relatively low CO emission of cold water diatoms (Gros

315   et al. 2009), since diatoms accounted for the large bloom at our shelf station 19 (Fig. 3).

Table 1: Mean values and standard deviation for trace gases concentrations in five different water masses along the transect (see Fig. S6 for exact areas), and from surface samples at eight sea-ice stations north of 80°N. S: salinity; BDL: below detection limit. *In italic: data from (Tran et al., 2013) during the ARK XXV expedition in the same area, but in June-July 2010, i.e. one month later in summer. Due to sensor 320 failure of temperature and salinity, the data start at 60°N.

	Acetonitrile (nM)	Acetaldehyde (nM)	Acetone (nM)	DMS (nM)	Methanethiol (nM)	Isoprene (pM)	CO (nM)
Coastal-influenced/low-salinity Atlantic Water (AWs; θ>5°C, S<34.4)	1.11 ± 0.55	19.67 ± 7.96	23.34 ± 12.77	15,65 ± 6.96	0.84 ± 0.65	2,55 ± 0.84 *23.4 ± 3.10**	10.70 ± 3.07 *2.50 ± 1.70**
warm Atlantic Water (wAW; θ>2°C, S>34.9)	0.53 ± 0.23	4.84 ± 4.03	2.36 ± 5.88	11,75 ± 6.97	2.89 ± 1.52	1,38 ± 0.70 *42.5 ± 49.6**	5.86 ± 2.77 *3.3± 2.2**
freshened Atlantic Water (fAW; θ>1°C, 34.4<S<34.9)	0.94 ± 0.40	9.84 ± 5.60	14.56 ± 10.80	13.05 ± 8.83	3.26 ± 1.49	2,66 ± 1.51 *24.8. ± 19.1**	10.17 ± 5.89 *3.4 ± 2.4**
cold Polar Water (cPW; θ<0°C, S<34.7)	0.32 ± 0.13	0.98 ± 2.27	BDL	30.03 ± 9.26	2.80 ± 0.76	1,22 ± 0.47	5.00 ± 2.82
warm Polar Water (wPW; θ>0°C, S<34.4)	0.21 ± 0.09	0.30 ± 0.86	BDL	34.65 ± 8.46	3.49 ± 0.29	1,06 ± 0.28	7.81 ± 2.08
Polar waters (PW) (cold+warm)	0.30 ± 0.13	0.84 ± 2.05	BDL	31.19 ± 9.29	2.96 ± 0.74	1,19 ± 0.44 *14.5 ± 11.5**	5.88 ± 2.91 *6.5 ± 3.2**
Surface water at sea-ice stations > 80ºN (range)	0.28±0.12 (0.15-0.47)	7.24±4.43 (0.27-14.23)	2.29±2.79 (0-6.93)	11.22±10.91 (1.64-31.90)	0.13±0.17 (0.02-0.53)	3.23±2.07 (0.90-7.25)	1.45±1.67 (0.24-4.26)

Considerable differences between Atlantic and polar waters were also evident for acetone, acetonitrile and acetaldehyde. Reference acetone data are scarce (Beale et al., 2013; Tanimoto et al., 2014; Wohl et al., 2020 and references therein), reporting

2 to 40 nm in the temperate and tropical Atlantic (Williams et al., 2004) as well as west Pacific Oceans (Marandino, 2005). In

325   the Atlantic Ocean, (Yang et al., 2014) have observed a mean value of 13.7 nM, without obvious correlation to biological activity. For the Arctic Yang et al., (2014) have reported 6.8 nM in the Labrador Sea and Wohl et al. (2019) 8 ± 2 nM in the Canadian Arctic, matching our data between 65-70°N. Notably, these patterns match the southern Atlantic at 60°S (Wohl et al., 2020), suggesting similar dynamics in both subpolar regions. For acetone, the ocean is considered to be both a photochemical source and a microbial sink depending on the region (Jacob et al., 2002; Fischer et al., 2012). This dual role

330   matches our records of relatively high values for latitudes up to 60°N, and values down to the detection limit in polar zones. For acetonitrile, the oceans are a comparatively small source (originating from phytoplankton) or sink (through bacteria consumption), depending on location and season (see Davie-Martin et al. (2020) and references therein). The concentrations measured in the present study were mostly >1 nM, and to our knowledge, the first reported in the Arctic Ocean. Overall, little is known about microbial utilization of acetone and acetonitrile, but biogenic effects have been suggested (Davie-Martin et al.

335   (2020). Correlations of NS9 with acetone and acetonitrile indicate an involvement in acetone and acetonitrile cycling among this diverse uncultured clade.

Prior acetaldehyde measurements (Zhou and Mopper, 1997; Kameyama et al., 2010; Yang et al., 2014) reported 1.5 to 5 nM in the North Atlantic Ocean. In the present study, concentrations in AWs (19.7 ± 8.0 nM) were on average twofold higher than those found by Yang et al. (2014) and Zhu and Kieber (2019) in the North Atlantic. However, these related studies measured

340   acetaldehyde in fall, which could explain the difference as the main source of acetaldehyde is attributed to photochemical degradation of CDOM. This corresponds to missing bacterial correlations with this compound.

4.2 DMS and MeSH

345   Previously reported DMS levels in polar oceans varied between 3 to 18 nM (Mungall et al., 2016; Jarníková et al., 2018; Uhlig et al., 2019), with up to 74 nM in the sub-surface Chl a maximum of the Baffin Bay (Galí et al., 2021). Hence, these are overall in the same range as our values. The average around 30 nM observed >80°N might be partly explained by the high DMS concentrations (up to 2000 nM) in sea ice (Levasseur, 2013). Indeed, ice-melt derived DMS can contribute up to 50% to the water column inventory (Tison et al., 2010).

350   As reviewed by Stefels et al. (2007), there is no direct relationship between DMS and Chl a on global scale, since the precursor of DMS, DMSP is produced by diverse phytoplankton at different rates, which vary with the physiological state. This notion corresponds to the missing correlation along our transect, where different phytoplankton types and bloom stages were observed (Spong et al. pers. comm.). However, in the vertical under-ice profiles, a strong correlation between Chl a and DMS was found in the Atlantic-influenced polar water masses, mirroring observations by Uhlig et al. (2019). Presumably, this

355   is a typical marginal sea ice zone effect, as found in other sectors of the Arctic (Galí and Simó, 2010; Levasseur, 2013; Park et al., 2013).

Compared to DMS, MeSH has seldom been quantified in marine waters to date, especially at polar latitudes. Leck and Rodhe (1991) have reported on average 0.16 nM MeSH in the Baltic Sea, and 0.28 nM and 0.34 nM in the North Sea respectively. Our data are one order of magnitude higher, ranging from 0.84 ± 0.65 nM in the AWs up to 3.49 nM in wPW,

360 i.e. in the same range observed by Kiene et al. (2017) in the northeast subarctic Pacific Ocean. These authors have shown that MeSH concentrations in surface waters generally decrease with depth, which overall matches our under-ice vertical profiles (although concentrations were low).

MeSH and DMS originate from the degradation of DMSP, mostly via bacterial demethylation (yielding MeSH) or cleavage (yielding DMS) pathways (Moran and Durham, 2019; Lawson et al., 2020 and references therein). Laboratory

365 experiments have indicated that the net yields of DMS and MeSH from DMSP were on average 32% and 22% respectively (Kiene, 1996). MeSH production might be promoted by low DMSP concentrations and high bacterial sulphur demand (Kilgour et al., 2022). Mesocosm experiments showed that the proportion of DMS versus MeSH increased from the pre-bloom phase to (induced) bloom conditions (Kilgour et al., 2022). In pelagic waters, DMS generally dominates gaseous sulphur, with MeSH being the second most abundant compound but contributing on average <10% to the total sulphur species in the North and

370 Baltic seas (Leck and Rodhe, 1991), in the Atlantic Ocean (Kettle et al., 2001), and in the Southwest Pacific Ocean (Lawson et al., 2020). Nevertheless, in some North Sea locations, MeSH contributed up to 40% (Leck and Rodhe, 1991), comparable to our measurements (Fig. 5) of 20-40% between 70°N-75°N and a maximum of 50% at 78.6°N. The overall MeSH contribution of 20% suggests that MeSH could represent a considerable fraction of sulphur, supported by the correlations of several bacterial genera. Correlations between *Yoonia-Loktanella* and *Ascidiaceihabitans* ASVs with MeSH reflected the

375 prominent role of *Rhodobacteraceae* in DMSP demethylation (Curson et al., 2011; Moran et al., 2012). The positive link of SAR11 and SUP05 ASVs corresponds to the prevalence of DMSP-metabolizing genes in these taxa (Nowinski et al., 2019; Landa et al., 2019; Sun et al., 2016). The link between cyanobacteria and MeSH was notable, since DMSP-utilizing genes appear to be rare in cyanobacteria (Liu et al., 2018). Hence, there might be indirect effects on other photosynthetic organisms, indicating yet undescribed chemical linkages among primary producers.
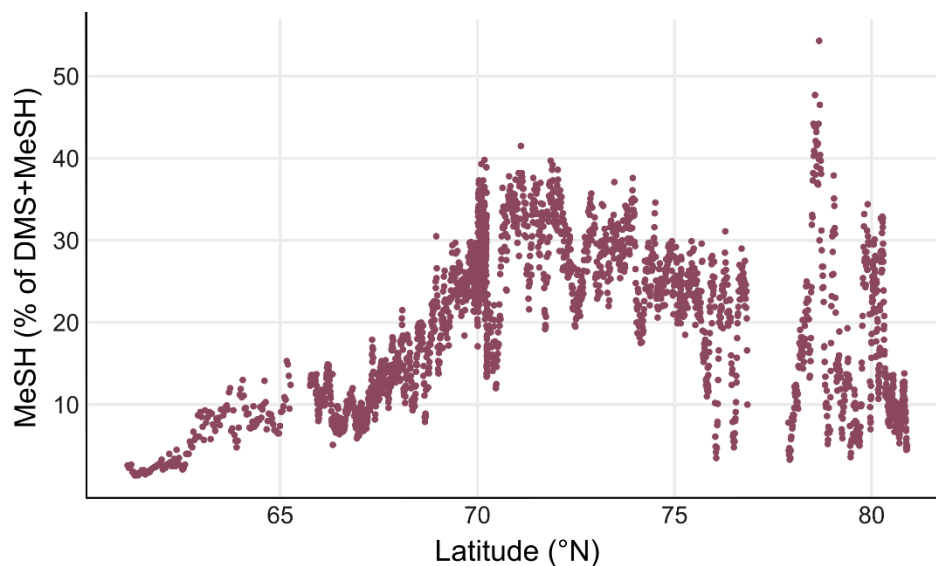
Fig. 5. Latitudinal variation of the MeSH fraction to the total sulphur compounds measured (DMS+MeSH)

5 Conclusion

We present the first measurements of DMS, MeSH and other trace gases along a transect from the North Atlantic to the ice-covered Arctic Ocean in spring 2015. High-resolution latitudinal data between 57°N and 80°N were complemented with vertical profiles at sea-ice stations >80°N. Whereas isoprene, acetone, acetaldehyde and acetonitrile concentrations decreased northwards, CO, DMS and MeSH were uncorrelated with latitude and retained considerable levels in polar waters. Hence, these probably have phytoplankton-driven origins with regional variability, e.g. through localized blooms. The peak of DMS in polar waters likely corresponded to sea ice as reservoir of DMS (Levasseur, 2013) and abundance of DMS-emitting phytoplankton. The marked correlation between DMS and Chl a in the diatom-dominated region >80°N represent a typical marginal sea ice zone effect. The missing correlation between DMS and MeSH suggested different processes of production and degradation, although they both originate from DMSP. Although DMS was overall more abundant, MeSH contributed on average 20% (and up to 50%) to the total DMS+MeSH budget, showing the importance to consider this trace gas as secondary aerosol producer in some regions. The potential importance of MeSH was underlined by more and stronger bacterial correlations with MeSH than DMS, illustrating the microbiological importance of DMSP demethylation across extensive latitudinal gradients. Notably, higher acetaldehyde concentrations >80°N suggests that ice-covered regions could be a reservoir of acetaldehyde. While artefacts from off-line measurements (sampling through Niskin bottles) cannot be completely excluded, this result indicates a potential role of this reactive compound in regional atmospheric chemistry. To further investigate marine trace gas dynamics, including the rapidly changing Arctic, further measurements in the different reservoirs (ocean, atmosphere, ice) are necessary. In conclusion, the shown patterns in trace gas concentrations in high spatial resolution provide important insights into climatically and biologically relevant compounds and their connection to microbiology.

17

Biogeosciences
Discussions

Open Access

EGU

References

Alvarez, L. A., Exton, D. A., Timmis, K. N., Suggett, D. J., and McGenity, T. J.: Characterization of marine isoprene-degrading communities, 11, 3280–3291, https://doi.org/10.1111/j.1462-2920.2009.02069.x, 2009.

405   von Appen, W.-J., Waite, A. M., Bergmann, M., Bienhold, C., Boebel, O., Bracher, A., Cisewski, B., Hagemann, J., Hoppema, M., Iversen, M. H., Konrad, C., Krumpen, T., Lochthofen, N., Metfies, K., Niehoff, B., Nöthig, E.-M., Purser, A., Salter, I., Schaber, M., Scholz, D., Soltwedel, T., Torres-Valdes, S., Wekerle, C., Wenzhöfer, F., Wietz, M., and Boetius, A.: Sea-ice derived meltwater stratification slows the biological carbon pump: results from continuous observations, Nat Commun, 12, 7309, https://doi.org/10.1038/s41467-021-26943-z, 2021.

Arrigo, K. R. and van Dijken, G. L.: Continued increases in Arctic Ocean primary production, Progress in Oceanography, 136,
410   60–70, https://doi.org/10.1016/j.pocean.2015.05.002, 2015.

Assmy, P., Fernández-Méndez, M., Duarte, P., Meyer, A., Randelhoff, A., Mundy, C. J., Olsen, L. M., Kauko, H. M., Bailey, A., Chierici, M., Cohen, L., Doulgeris, A. P., Ehn, J. K., Fransson, A., Gerland, S., Hop, H., Hudson, S. R., Hughes, N., Itkin, P., Johnsen, G., King, J. A., Koch, B. P., Koenig, Z., Kwasniewski, S., Laney, S. R., Nicolaus, M., Pavlov, A. K., Polashenski, C. M., Provost, C., Rösel, A., Sandbu, M., Spreen, G., Smedsrud, L. H., Sundfjord, A., Taskjelle, T., Tatarek, A., Wiktor, J.,
415   Wagner, P. M., Wold, A., Steen, H., and Granskog, M. A.: Leads in Arctic pack ice enable early phytoplankton blooms below snow-covered sea ice, Sci Rep, 7, 40850, https://doi.org/10.1038/srep40850, 2017.

Beale, R., Dixon, J. L., Arnold, S. R., Liss, P. S., and Nightingale, P. D.: Methanol, acetaldehyde, and acetone in the surface waters of the Atlantic Ocean: OVOCs in The Atlantic Ocean, J. Geophys. Res. Oceans, 118, 5412–5425, https://doi.org/10.1002/jgrc.20322, 2013.

420   Bikkina, S., Kawamura, K., Miyazaki, Y., and Fu, P.: High abundances of oxalic, azelaic, and glyoxylic acids and methylglyoxal in the open ocean with high biological activity: Implication for secondary OA formation from isoprene: Oceanic control on atmospheric SOA, Geophys. Res. Lett., 41, 3649–3657, https://doi.org/10.1002/2014GL059913, 2014.

Blake, R. S., Monks, P. S., and Ellis, A. M.: Proton-Transfer Reaction Mass Spectrometry, Chem. Rev., 109, 861–896, https://doi.org/10.1021/cr800364q, 2009.

425   Bonsang, B., Polle, C., and Lambert, G.: Evidence for marine production of isoprene, Geophys. Res. Lett., 19, 1129–1132, https://doi.org/10.1029/92GL00083, 1992.

Bonsang, B., Gros, V., Peeken, I., Yassaa, N., Bluhm, K., Zoellner, E., Sarda-Esteve, R., and Williams, J.: Isoprene emission from phytoplankton monocultures: the relationship with chlorophyll-a, cell volume and carbon content, Environ. Chem., 7, 554, https://doi.org/10.1071/EN09156, 2010.

430   Callahan, B. J., McMurdie, P. J., Rosen, M. J., Han, A. W., Johnson, A. J. A., and Holmes, S. P.: DADA2: High-resolution sample inference from Illumina amplicon data, Nat Methods, 13, 581–583, https://doi.org/10.1038/nmeth.3869, 2016.

Campen, H. I., Arévalo-Martínez, D. L., Artioli, Y., Brown, I. J., Kitidis, V., Lessin, G., Rees, A. P., and Bange, H. W.: The role of a changing Arctic Ocean and climate for the biogeochemical cycling of dimethyl sulphide and carbon monoxide, Ambio, 51, 411–422, https://doi.org/10.1007/s13280-021-01612-z, 2022.

435   Carrión, O., McGenity, T. J., and Murrell, J. C.: Molecular Ecology of Isoprene-Degrading Bacteria, Microorganisms, 8, 967, https://doi.org/10.3390/microorganisms8070967, 2020.

Conte, L., Szopa, S., Séférian, R., and Bopp, L.: The oceanic cycle of carbon monoxide and its emissions to the atmosphere, Biogeosciences, 16, 881–902, https://doi.org/10.5194/bg-16-881-2019, 2019.

440 Curson, A. R. J., Todd, J. D., Sullivan, M. J., and Johnston, A. W. B.: Catabolism of dimethylsulphoniopropionate: microorganisms, enzymes and genes, Nat Rev Microbiol, 9, 849–859, https://doi.org/10.1038/nrmicro2653, 2011.

Davie-Martin, C. L., Giovannoni, S. J., Behrenfeld, M. J., Penta, W. B., and Halsey, K. H.: Seasonal and Spatial Variability in the Biogenic Production and Consumption of Volatile Organic Compounds (VOCs) by Marine Plankton in the North Atlantic Ocean, Front. Mar. Sci., 7, 611870, https://doi.org/10.3389/fmars.2020.611870, 2020.

Degerlund, M. and Eilertsen, H. C.: Main Species Characteristics of Phytoplankton Spring Blooms in NE Atlantic and Arctic
445 Waters (68–80° N), Estuaries and Coasts, 33, 242–269, https://doi.org/10.1007/s12237-009-9167-7, 2010.

Duncan, B. N., Logan, J. A., Bey, I., Megretskaia, I. A., Yantosca, R. M., Novelli, P. C., Jones, N. B., and Rinsland, C. P.: Global budget of CO, 1988–1997: Source estimates and validation with a global model, J. Geophys. Res., 112, D22301, https://doi.org/10.1029/2007JD008459, 2007.

Dybwad, C., Assmy, P., Olsen, L. M., Peeken, I., Nikolopoulos, A., Krumpen, T., Randelhoff, A., Tatarek, A., Wiktor, J. M.,
450 and Reigstad, M.: Carbon Export in the Seasonal Sea Ice Zone North of Svalbard From Winter to Late Summer, Front. Mar. Sci., 7, 525800, https://doi.org/10.3389/fmars.2020.525800, 2021.

Fernández-Méndez, M., Wenzhöfer, F., Peeken, I., Sørensen, H. L., Glud, R. N., and Boetius, A.: Composition, Buoyancy Regulation and Fate of Ice Algal Aggregates in the Central Arctic Ocean, PLoS ONE, 9, e107452, https://doi.org/10.1371/journal.pone.0107452, 2014.

455 Fischer, E. V., Jacob, D. J., Millet, D. B., Yantosca, R. M., and Mao, J.: The role of the ocean in the global atmospheric budget of acetone: ATMOSPHERIC BUDGET OF ACETONE, Geophys. Res. Lett., 39, n/a-n/a, https://doi.org/10.1029/2011GL050086, 2012.

Galí, M. and Simó, R.: Occurrence and cycling of dimethylated sulfur compounds in the Arctic during summer receding of the ice edge, Marine Chemistry, 122, 105–117, https://doi.org/10.1016/j.marchem.2010.07.003, 2010.

460 Galí, M., Lizotte, M., Kieber, D. J., Randelhoff, A., Hussherr, R., Xue, L., Dinasquet, J., Babin, M., Rehm, E., and Levasseur, M.: DMS emissions from the Arctic marginal ice zone, 9, 00113, https://doi.org/10.1525/elementa.2020.00113, 2021.

Gros, V., Bonsang, B., and Sarda Esteve, R.: Atmospheric carbon monoxide 'in situ' monitoring by automatic gas chromatography, Chemosphere - Global Change Science, 1, 153–161, https://doi.org/10.1016/S1465-9972(99)00010-0, 1999.

Gros, V., Peeken, I., Bluhm, K., Zöllner, E., Sarda-Esteve, R., and Bonsang, B.: Carbon monoxide emissions by phytoplankton:
465 evidence from laboratory experiments, Environ. Chem., 6, 369, https://doi.org/10.1071/EN09020, 2009.

Guenther, A., Hewitt, C. N., Erickson, D., Fall, R., Geron, C., Graedel, T., Harley, P., Klinger, L., Lerdau, M., Mckay, W. A., Pierce, T., Scholes, B., Steinbrecher, R., Tallamraju, R., Taylor, J., and Zimmerman, P.: A global model of natural volatile organic compound emissions, J. Geophys. Res., 100, 8873, https://doi.org/10.1029/94JD02950, 1995.

Hackenberg, S. C., Andrews, S. J., Airs, R., Arnold, S. R., Bouman, H. A., Brewin, R. J. W., Chance, R. J., Cummings, D.,
470 Dall'Olmo, G., Lewis, A. C., Minaeian, J. K., Reifel, K. M., Small, A., Tarran, G. A., Tilstone, G. H., and Carpenter, L. J.: Potential controls of isoprene in the surface ocean: Isoprene Controls in the Surface Ocean, Global Biogeochem. Cycles, 31, 644–662, https://doi.org/10.1002/2016GB005531, 2017.

Biogeosciences
Discussions
Open Access
EGU

Hegseth, E. N. and Sundfjord, A.: Intrusion and blooming of Atlantic phytoplankton species in the high Arctic, Journal of Marine Systems, 74, 108–119, https://doi.org/10.1016/j.jmarsys.2007.11.011, 2008.

475 Jacob, D. J., Field, B. D., Jin, E. M., Bey, I., Li, Q., Logan, J. A., Yantosca, R. M., and Singh, H. B.: Atmospheric budget of acetone: ATMOSPHERIC BUDGET OF ACETONE, J. Geophys. Res., 107, ACH 5-1-ACH 5-17, https://doi.org/10.1029/2001JD000694, 2002.

Jarníková, T., Dacey, J., Lizotte, M., Levasseur, M., and Tortell, P.: The distribution of methylated sulfur compounds, DMS and DMSP, in Canadian subarctic and Arctic marine waters during summer 2015, Biogeosciences, 15, 2449–2465, 480 https://doi.org/10.5194/bg-15-2449-2018, 2018.

Kameyama, S., Tanimoto, H., Inomata, S., Tsunogai, U., Ooki, A., Takeda, S., Obata, H., Tsuda, A., and Uematsu, M.: High-resolution measurement of multiple volatile organic compounds dissolved in seawater using equilibrator inlet–proton transfer reaction-mass spectrometry (EI–PTR-MS), Marine Chemistry, 122, 59–73, https://doi.org/10.1016/j.marchem.2010.08.003, 2010.

485 Kansal, A.: Sources and reactivity of NMHCs and VOCs in the atmosphere: A review, Journal of Hazardous Materials, 166, 17–26, https://doi.org/10.1016/j.jhazmat.2008.11.048, 2009.

Kettle, A. J., Rhee, T. S., von Hobe, M., Poulton, A., Aiken, J., and Andreae, M. O.: Assessing the flux of different volatile sulfur gases from the ocean to the atmosphere, J. Geophys. Res., 106, 12193–12209, https://doi.org/10.1029/2000JD900630, 2001.

490 Kiene, R. P.: Production of methanethiol from dimethylsulfoniopropionate in marine surface waters, Marine Chemistry, 54, 69–83, https://doi.org/10.1016/0304-4203(96)00006-0, 1996.

Kiene, R. P., Willams T.E., Esson, K., Tortell, P., and Dacey, J.W. H.: Concentrations and Sea-Air Fluxes in the Subarctic NE Pacific Ocean, AGU, Fall Meeting, San Francisco, 2017.

Kilgour, D. B., Novak, G. A., Sauer, J. S., Moore, A. N., Dinasquet, J., Amiri, S., Franklin, E. B., Mayer, K., Winter, M., 495 Morris, C. K., Price, T., Malfatti, F., Crocker, D. R., Lee, C., Cappa, C. D., Goldstein, A. H., Prather, K. A., and Bertram, T. H.: Marine gas-phase sulfur emissions during an induced phytoplankton bloom, Atmos. Chem. Phys., 22, 1601–1613, https://doi.org/10.5194/acp-22-1601-2022, 2022.

Landa, M., Burns, A. S., Durham, B. P., Esson, K., Nowinski, B., Sharma, S., Vorobev, A., Nielsen, T., Kiene, R. P., and Moran, M. A.: Sulfur metabolites that facilitate oceanic phytoplankton–bacteria carbon flux, ISME J, 13, 2536–2550, 500 https://doi.org/10.1038/s41396-019-0455-3, 2019.

Lannuzel, D., Tedesco, L., van Leeuwe, M., Campbell, K., Flores, H., Delille, B., Miller, L., Stefels, J., Assmy, P., Bowman, J., Brown, K., Castellani, G., Chierici, M., Crabeck, O., Damm, E., Else, B., Fransson, A., Fripiat, F., Geilfus, N.-X., Jacques, C., Jones, E., Kaartokallio, H., Kotovitch, M., Meiners, K., Moreau, S., Nomura, D., Peeken, I., Rintala, J.-M., Steiner, N., Tison, J.-L., Vancoppenolle, M., Van der Linden, F., Vichi, M., and Wongpan, P.: The future of Arctic sea-ice biogeochemistry 505 and ice-associated ecosystems, Nat. Clim. Chang., 10, 983–992, https://doi.org/10.1038/s41558-020-00940-4, 2020.

Lawson, S. J., Law, C. S., Harvey, M. J., Bell, T. G., Walker, C. F., de Bruyn, W. J., and Saltzman, E. S.: Methanethiol, dimethyl sulfide and acetone over biologically productive waters in the southwest Pacific Ocean, Atmos. Chem. Phys., 20, 3061–3078, https://doi.org/10.5194/acp-20-3061-2020, 2020.

Leck, C. and Rodhe, H.: Emissions of marine biogenic sulfur to the atmosphere of northern Europe, J Atmos Chem, 12, 63– 510 86, https://doi.org/10.1007/BF00053934, 1991.

20

Levasseur, M.: Impact of Arctic meltdown on the microbial cycling of sulphur, Nature Geosci, 6, 691–700, https://doi.org/10.1038/ngeo1910, 2013.

Lindinger, W. and Jordan, A.: Proton-transfer-reaction mass spectrometry (PTR–MS): on-line monitoring of volatile organic compounds at pptv levels, Chem. Soc. Rev., 27, 347, https://doi.org/10.1039/a827347z, 1998.

515   Liu, J., Liu, J., Zhang, S.-H., Liang, J., Lin, H., Song, D., Yang, G.-P., Todd, J. D., and Zhang, X.-H.: Novel Insights Into Bacterial Dimethylsulfoniopropionate Catabolism in the East China Sea, Front. Microbiol., 9, 3206, https://doi.org/10.3389/fmicb.2018.03206, 2018.

Love, C. R., Arrington, E. C., Gosselin, K. M., Reddy, C. M., Van Mooy, B. A. S., Nelson, R. K., and Valentine, D. L.: Microbial production and consumption of hydrocarbons in the global ocean, Nat Microbiol, 6, 489–498, 520   https://doi.org/10.1038/s41564-020-00859-8, 2021.

Marandino, C. A.: Oceanic uptake and the global atmospheric acetone budget, Geophys. Res. Lett., 32, L15806, https://doi.org/10.1029/2005GL023285, 2005.

Martin, M.: Cutadapt removes adapter sequences from high-throughput sequencing reads, EMBnet j., 17, 10, https://doi.org/10.14806/ej.17.1.200, 2011.

525   Massicotte, P., Peeken, I., Katlein, C., Flores, H., Huot, Y., Castellani, G., Arndt, S., Lange, B. A., Tremblay, J., and Babin, M.: Sensitivity of Phytoplankton Primary Production Estimates to Available Irradiance Under Heterogeneous Sea Ice Conditions, J. Geophys. Res. Oceans, 124, 5436–5450, https://doi.org/10.1029/2019JC015007, 2019.

Metfies, K., Schroeder, F., Hessel, J., Wollschläger, J., Micheller, S., Wolf, C., Kilias, E., Sprong, P., Neuhaus, S., Frickenhaus, S., and Petersen, W.: High-resolution monitoring of marine protists based on an observation strategy integrating automated 530   on-board filtration and molecular analyses, Ocean Sci., 12, 1237–1247, https://doi.org/10.5194/os-12-1237-2016, 2016.

Metfies, K., Hessel, J., Klenk, R., Petersen, W., Wiltshire, K. H., and Kraberg, A.: Uncovering the intricacies of microbial community dynamics at Helgoland Roads at the end of a spring bloom using automated sampling and 18S meta-barcoding, PLoS ONE, 15, e0233921, https://doi.org/10.1371/journal.pone.0233921, 2020.

Moran, M. A. and Durham, B. P.: Sulfur metabolites in the pelagic ocean, Nat Rev Microbiol, 17, 665–678, 535   https://doi.org/10.1038/s41579-019-0250-1, 2019.

Moran, M. A., Reisch, C. R., Kiene, R. P., and Whitman, W. B.: Genomic Insights into Bacterial DMSP Transformations, Annu. Rev. Mar. Sci., 4, 523–542, https://doi.org/10.1146/annurev-marine-120710-100827, 2012.

Mungall, E. L., Croft, B., Lizotte, M., Thomas, J. L., Murphy, J. G., Levasseur, M., Martin, R. V., Wentzell, J. J. B., Liggio, J., and Abbatt, J. P. D.: Dimethyl sulfide in the summertime Arctic atmosphere: measurements and source sensitivity 540   simulations, Atmos. Chem. Phys., 16, 6665–6680, https://doi.org/10.5194/acp-16-6665-2016, 2016.

Nikolopoulos, Anna, Janout, Markus A, Hölemann, Jens A, Juhls, Bennet, Korhonen, Meri, and Randelhoff, Achim: Physical oceanography measured on water bottle samples during POLARSTERN cruise PS92 (ARK-XXIX/1), https://doi.org/10.1594/PANGAEA.861866, 2016.

Nöthig, E.-M., Bracher, A., Engel, A., Metfies, K., Niehoff, B., Peeken, I., Bauerfeind, E., Cherkasheva, A., Gäbler-Schwarz, 545   S., Hardge, K., Kilias, E., Kraft, A., Mebrahtom Kidane, Y., Lalande, C., Piontek, J., Thomisch, K., and Wurst, M.: Summertime plankton ecology in Fram Strait—a compilation of long- and short-term observations, Polar Research, 34, 23349, https://doi.org/10.3402/polar.v34.23349, 2015.

Novak, G. A., Kilgour, D. B., Jernigan, C. M., Vermeuel, M. P., and Bertram, T. H.: Oceanic emissions of dimethyl sulfide and methanethiol and their contribution to sulfur dioxide production in the marine atmosphere, Gases/Field 550 Measurements/Troposphere/Chemistry (chemical composition and reactions), https://doi.org/10.5194/acp-2021-891, 2021.

Nowinski, B., Motard-Côté, J., Landa, M., Preston, C. M., Scholin, C. A., Birch, J. M., Kiene, R. P., and Moran, M. A.: Microdiversity and temporal dynamics of marine bacterial dimethylsulfoniopropionate genes, Environ Microbiol, 21, 1687–1701, https://doi.org/10.1111/1462-2920.14560, 2019.

Ooki, A., Nomura, D., Nishino, S., Kikuchi, T., and Yokouchi, Y.: A global-scale map of isoprene and volatile organic iodine 555 in surface seawater of the A rctic, N orthwest P acific, I ndian, and S outhern O ceans, J. Geophys. Res. Oceans, 120, 4108–4128, https://doi.org/10.1002/2014JC010519, 2015.

Parada, A. E., Needham, D. M., and Fuhrman, J. A.: Every base matters: assessing small subunit rRNA primers for marine microbiomes with mock communities, time series and global field samples: Primers for marine microbiome studies, Environ Microbiol, 18, 1403–1414, https://doi.org/10.1111/1462-2920.13023, 2016.

560 Park, K.-T., Lee, K., Yoon, Y.-J., Lee, H.-W., Kim, H.-C., Lee, B.-Y., Hermansen, O., Kim, T.-W., and Holmén, K.: Linking atmospheric dimethyl sulfide and the Arctic Ocean spring bloom: ATMOSPHERIC DMS IN THE ARCTIC SPRING BLOOM, Geophys. Res. Lett., 40, 155–160, https://doi.org/10.1029/2012GL054560, 2013.

Peeken, I.: The Expedition PS92 of the Research Vessel Polarstern to the Arctic Ocean in 2015, Alfred-Wegener-Institut, Helmholtz-Zentrum für Polar- und Meeresforschung, https://doi.org/10.2312/BZPM_0694_2016, 2016.

565 Petersen, W.: FerryBox systems: State-of-the-art in Europe and future development, Journal of Marine Systems, 140, 4–12, https://doi.org/10.1016/j.jmarsys.2014.07.003, 2014.

Polyakov, I. V., Alkire, M. B., Bluhm, B. A., Brown, K. A., Carmack, E. C., Chierici, M., Danielson, S. L., Ellingsen, I., Ershova, E. A., Gårdfeldt, K., Ingvaldsen, R. B., Pnyushkov, A. V., Slagstad, D., and Wassmann, P.: Borealization of the Arctic Ocean in Response to Anomalous Advection From Sub-Arctic Seas, Front. Mar. Sci., 7, 491, 570 https://doi.org/10.3389/fmars.2020.00491, 2020.

Quast, C., Pruesse, E., Yilmaz, P., Gerken, J., Schweer, T., Yarza, P., Peplies, J., and Glöckner, F. O.: The SILVA ribosomal RNA gene database project: improved data processing and web-based tools, 41, D590–D596, https://doi.org/10.1093/nar/gks1219, 2012.

Schmale, J., Zieger, P., and Ekman, A. M. L.: Aerosols in current and future Arctic climate, Nat. Clim. Chang., 11, 95–105, 575 https://doi.org/10.1038/s41558-020-00969-5, 2021.

Shaw, S. L., Gantt, B., and Meskhidze, N.: Production and Emissions of Marine Isoprene and Monoterpenes: A Review, Advances in Meteorology, 2010, 1–24, https://doi.org/10.1155/2010/408696, 2010.

Simó, R., Cortés-Greus, P., Rodríguez-Ros, P., and Masdeu-Navarro, M.: Substantial loss of isoprene in the surface ocean due to chemical and biological consumption, Commun Earth Environ, 3, 20, https://doi.org/10.1038/s43247-022-00352-6, 2022.

580 Skagseth, Ø., Broms, C., Gundersen, K., Hátún, H., Kristiansen, I., Larsen, K. M. H., Mork, K. A., Petursdottir, H., and Søiland, H.: Arctic and Atlantic Waters in the Norwegian Basin, Between Year Variability and Potential Ecosystem Implications, Front. Mar. Sci., 9, 831739, https://doi.org/10.3389/fmars.2022.831739, 2022.

Song, G., Xie, H., Aubry, C., Zhang, Y., Gosselin, M., Mundy, C. J., Philippe, B., and Papakyriakou, T. N.: Spatiotemporal variations of dissolved organic carbon and carbon monoxide in first-year sea ice in the western Canadian Arctic, J. Geophys. Res., 116, C00G05, https://doi.org/10.1029/2010JC006867, 2011.

Stefels, J., Steinke, M., Turner, S., Malin, G., and Belviso, S.: Environmental constraints on the production and removal of the climatically active gas dimethylsulphide (DMS) and implications for ecosystem modelling, Biogeochemistry, 83, 245–275, https://doi.org/10.1007/s10533-007-9091-5, 2007.

Sun, J., Todd, J. D., Thrash, J. C., Qian, Y., Qian, M. C., Temperton, B., Guo, J., Fowler, E. K., Aldrich, J. T., Nicora, C. D., Lipton, M. S., Smith, R. D., De Leenheer, P., Payne, S. H., Johnston, A. W. B., Davie-Martin, C. L., Halsey, K. H., and Giovannoni, S. J.: The abundant marine bacterium Pelagibacter simultaneously catabolizes dimethylsulfoniopropionate to the gases dimethyl sulfide and methanethiol, Nat Microbiol, 1, 16065, https://doi.org/10.1038/nmicrobiol.2016.65, 2016.

Sunagawa, S., Coelho, L. P., Chaffron, S., Kultima, J. R., Labadie, K., Salazar, G., Djahanschiri, B., Zeller, G., Mende, D. R., Alberti, A., Cornejo-Castillo, F. M., Costea, P. I., Cruaud, C., d'Ovidio, F., Engelen, S., Ferrera, I., Gasol, J. M., Guidi, L., Hildebrand, F., Kokoszka, F., Lepoivre, C., Lima-Mendez, G., Poulain, J., Poulos, B. T., Royo-Llonch, M., Sarmento, H., Vieira-Silva, S., Dimier, C., Picheral, M., Searson, S., Kandels-Lewis, S., Tara Oceans coordinators, Bowler, C., de Vargas, C., Gorsky, G., Grimsley, N., Hingamp, P., Iudicone, D., Jaillon, O., Not, F., Ogata, H., Pesant, S., Speich, S., Stemmann, L., Sullivan, M. B., Weissenbach, J., Wincker, P., Karsenti, E., Raes, J., Acinas, S. G., Bork, P., Boss, E., Bowler, C., Follows, M., Karp-Boss, L., Krzic, U., Reynaud, E. G., Sardet, C., Sieracki, M., and Velayoudon, D.: Structure and function of the global ocean microbiome, Science, 348, 1261359, https://doi.org/10.1126/science.1261359, 2015.

Tanimoto, H., Kameyama, S., Omori, Y., Inomata, S., and Tsunogai, U.: High-Resolution Measurement of Volatile Organic Compounds Dissolved in Seawater Using Equilibrator Inlet-Proton Transfer Reaction-Mass Spectrometry (EI-PTR-MS), in: Western Pacific Air-Sea Interaction Study, edited by: Uematsu, M., Yokouchi, Y., Watanabe, Y., Takeda, S., and Yamanaka, Y., TERRAPUB, 89–115, https://doi.org/10.5047/w-pass.a02.001, 2014.

Thompson, H. F., Summers, S., Yuecel, R., and Gutierrez, T.: Hydrocarbon-Degrading Bacteria Found Tightly Associated with the 50–70 µm Cell-Size Population of Eukaryotic Phytoplankton in Surface Waters of a Northeast Atlantic Region, Microorganisms, 8, 1955, https://doi.org/10.3390/microorganisms8121955, 2020.

Tison, J.-L., Brabant, F., Dumont, I., and Stefels, J.: High-resolution dimethyl sulfide and dimethylsulfoniopropionate time series profiles in decaying summer first-year sea ice at Ice Station Polarstern, western Weddell Sea, Antarctica, J. Geophys. Res., 115, G04044, https://doi.org/10.1029/2010JG001427, 2010.

Tolli, J. D. and Taylor, C. D.: Biological CO oxidation in the Sargasso Sea and in Vineyard Sound, Massachusetts, Limnol. Oceanogr., 50, 1205–1212, https://doi.org/10.4319/lo.2005.50.4.1205, 2005.

Tran, S., Bonsang, B., Gros, V., Peeken, I., Sarda-Esteve, R., Bernhardt, A., and Belviso, S.: A survey of carbon monoxide and non-methane hydrocarbons in the Arctic Ocean during summer 2010, Biogeosciences, 10, 1909–1935, https://doi.org/10.5194/bg-10-1909-2013, 2013.

Uhlig, C., Damm, E., Peeken, I., Krumpen, T., Rabe, B., Korhonen, M., and Ludwichowski, K.-U.: Sea Ice and Water Mass Influence Dimethylsulfide Concentrations in the Central Arctic Ocean, Front. Earth Sci., 7, 179, https://doi.org/10.3389/feart.2019.00179, 2019.

Wang, S., Hornbrook, R. S., Hills, A., Emmons, L. K., Tilmes, S., Lamarque, J., Jimenez, J. L., Campuzano-Jost, P., Nault, B. A., Crounse, J. D., Wennberg, P. O., Kim, M., Allen, H., Ryerson, T. B., Thompson, C. R., Peischl, J., Moore, F., Nance, D., Hall, B., Elkins, J., Tanner, D., Huey, L. G., Hall, S. R., Ullmann, K., Orlando, J. J., Tyndall, G. S., Flocke, F. M., Ray, E., Hanisco, T. F., Wolfe, G. M., St. Clair, J., Commane, R., Daube, B., Barletta, B., Blake, D. R., Weinzierl, B., Dollner, M.,

Conley, A., Vitt, F., Wofsy, S. C., Riemer, D. D., and Apel, E. C.: Atmospheric Acetaldehyde: Importance of Air-Sea Exchange and a Missing Source in the Remote Troposphere, Geophys. Res. Lett., 46, 5601–5613, https://doi.org/10.1029/2019GL082034, 2019.

625

Williams, J., Holzinger, R., Gros, V., Xu, X., Atlas, E., and Wallace, D. W. R.: Measurements of organic species in air and seawater from the tropical Atlantic: ORGANIC SPECIES IN AIR AND SEA, Geophys. Res. Lett., 31, https://doi.org/10.1029/2004GL020012, 2004.

Wilson, D. F., Swinnerton, J. W., and Lamontagne, R. A.: Production of Carbon Monoxide and Gaseous Hydrocarbons in
630 Seawater: Relation to Dissolved Organic Carbon, Science, 168, 1577–1579, https://doi.org/10.1126/science.168.3939.1577, 1970.

Wohl, C., Capelle, D., Jones, A., Sturges, W. T., Nightingale, P. D., Else, B. G. T., and Yang, M.: Segmented flow coil equilibrator coupled to a proton-transfer-reaction mass spectrometer for measurements of a broad range of volatile organic compounds in seawater, Ocean Sci., 15, 925–940, https://doi.org/10.5194/os-15-925-2019, 2019.

635 Wohl, C., Brown, I., Kitidis, V., Jones, A. E., Sturges, W. T., Nightingale, P. D., and Yang, M.: Underway seawater and atmospheric measurements of volatile organic compounds in the Southern Ocean, Biogeosciences, 17, 2593–2619, https://doi.org/10.5194/bg-17-2593-2020, 2020.

Wollenburg, J. E., Katlein, C., Nehrke, G., Nöthig, E.-M., Matthiessen, J., Wolf- Gladrow, D. A., Nikolopoulos, A., Gázquez-Sanchez, F., Rossmann, L., Assmy, P., Babin, M., Bruyant, F., Beaulieu, M., Dybwad, C., and Peeken, I.: Ballasting by
640 cryogenic gypsum enhances carbon export in a Phaeocystis under-ice bloom, Sci Rep, 8, 7703, https://doi.org/10.1038/s41598-018-26016-0, 2018.

Xie, H. and Gosselin, M.: Photoproduction of carbon monoxide in first-year sea ice in Franklin Bay, southeastern Beaufort Sea: PHOTOPRODUCTION OF CO IN SEA ICE, Geophys. Res. Lett., 32, n/a-n/a, https://doi.org/10.1029/2005GL022803, 2005.

645 Xie, H. and Zafiriou, O. C.: Evidence for significant photochemical production of carbon monoxide by particles in coastal and oligotrophic marine waters, Geophys. Res. Lett., 36, L23606, https://doi.org/10.1029/2009GL041158, 2009.

Yang, M., Beale, R., Liss, P., Johnson, M., Blomquist, B., and Nightingale, P.: Air–sea fluxes of oxygenated volatile organic compounds across the Atlantic Ocean, Atmos. Chem. Phys., 14, 7499–7517, https://doi.org/10.5194/acp-14-7499-2014, 2014.

Zhou, X. and Mopper, K.: Photochemical production of low-molecular-weight carbonyl compounds in seawater and surface
650 microlayer and their air-sea exchange, Marine Chemistry, 56, 201–213, https://doi.org/10.1016/S0304-4203(96)00076-X, 1997.

Zhu, Y. and Kieber, D. J.: Concentrations and Photochemistry of Acetaldehyde, Glyoxal, and Methylglyoxal in the Northwest Atlantic Ocean, Environ. Sci. Technol., 53, 9512–9521, https://doi.org/10.1021/acs.est.9b01631, 2019.

655

Biogeosciences
Discussions

Author contributions

VG, RSE, BB, and IP designed the study. BB, VG and RSE performed trace gas measurements prior to the campaign; VG and
660   RSE performed trace gas measurements on-board. IP coordinated all TRANSSIZ work, supervised the biological sampling
on-board and subsequent performed pigments analyses. AN coordinated the oceanographic sampling and water mass
classification. KM set up the AUTOFIM sampling system and supervised DNA extraction. MW performed bacterial
community analyses. VG, BB, IP and MW wrote the manuscript. All co-authors have read and commented the manuscript.

Competing interests

665

The authors declare no competing interests.

Acknowledgments